

Spiral patterns in planetesimal circumbinary disks

Tatiana V. Demidova, Ivan I. Shevchenko*
Pulkovo Observatory of the Russian Academy of Sciences
Pulkovskoje ave. 65, St. Petersburg 196140, Russia

Abstract

Planet formation scenarios and the observed planetary dynamics in binaries pose a number of theoretical challenges, especially in what concerns circumbinary planetary systems. We explore the dynamical stirring of a planetesimal circumbinary disk in the epoch when the gas component disappears. For this purpose, following theoretical approaches by Heppenheimer (1978) and Moriwaki & Nakagawa (2004), we develop a secular theory for the dynamics of planetesimals in circumbinary disks. If the binary is eccentric and its components have unequal masses, a spiral density wave is generated, engulfing the disk on the secular timescale. This spiral pattern is transient; thus its observed presence may betray system's young age. We explore the pattern both analytically and in numeric experiments. The derived analytical spiral is a modified *lituus*; it matches the numeric density wave in the gas-free case perfectly. Using the SPH scheme, we explore the effect of residual gas on the wave propagation.

Key words: binary stars – exoplanets – planetesimals – astrophysical disks – circumbinary planetary systems.

*E-mail: iis@gao.spb.ru

1 Introduction

Planet formation scenarios and the observed planetary dynamics in binaries pose a number of theoretical challenges, especially in what concerns circumbinary planetary systems. The orbital motion of the central binary induces formation of global structures in the gas-dust protoplanetary disk. In particular, a cavity is formed in the central part of the circumbinary disk; though, the cavity can be penetrated by streams of matter, maintaining the accretion activity of the binary components. Numerical simulations of the gas accretion in such systems were performed in (Artymowicz & Lubow, 1996; Bate & Bonnell, 1997; Sotnikova & Grinin, 2007) using the SPH method, and in (Gunther & Kley, 2002; Ochi et al., 2005; Hanawa et al., 2010; Kaigorodov et al., 2010) using finite-difference schemes. If the masses of the binary components are comparable (i.e., the mass ratio is greater than ~ 0.1), spiral patterns usually form, spreading inwards from the circumbinary disk to the circumstellar disks of the components. If the binary is moderately-sized ($4 < a_b < 30$ AU), the circumstellar disks of the components are still strongly perturbed (Nelson, 2000). Spiral arms form in the disk around the primary component due to the eccentric motion of the secondary; the structure depends on the orbital period and other parameters of the binary (Kley & Nelson, 2008; Paardekooper et al., 2008; Marzari et al., 2009). Models of radiative disks are considered in (Marzari et al., 2012; Picogna & Marzari, 2013); in such models, the spiral waves appear more damped and smooth.

Spiral density waves may as well emerge in the inner regions of cool accretion disks around components of semidetached binary systems. The possibility of observations of such patterns, obtained in three-dimensional gas-dynamical simulations, was discussed in Bisikalo et al. (2004). In this case, the pattern formation is due to the differential orbital precession of the accreting particles; this precession is caused by perturbations from the donor star.

It is known that a spiral wave can form in the planetesimal disk, if the disturbing body is a planet (Wyatt, 2005; Mustill & Wyatt, 2009; Matthews et al., 2014). Wyatt (2005) showed that a tightly wound spiral starts to propagate through the disk, if a planet is introduced in it. As in the theory of Bisikalo et al. (2004), the spiral is generated by differential precession between neighbouring particle orbits. To estimate the perturbation effect of a planet on the orbits of planetesimals, Wyatt (2005) considered the variation of the complex eccentricity coupled with the variation of the longitude

of pericenter, using Lagrange’s planetary equations. He used this secular theory of precessing planetesimal orbits to explain a spiral pattern resolved in Clampin et al. (2003) in the image of the HD 141569 disk; a comparison of the analytical theory and simulations of the secular perturbations in the planetesimal disk by a giant planet was performed. An important effect, considered by Mustill & Wyatt (2009), is the dynamical heating of the disk as a result of the spiral wave propagation, caused by a planet introduced in the disk: the planetesimal velocity dispersion increases. This phenomenon, hindering the planetesimal coalescence, may effect the further process of planetary formation. Of course, in the considered below case of a disk around a binary star a similar effect may be even of greater importance.

The protoplanetary disks radiate in the infrared and submillimeter spectral ranges, because the disks contain small-sized dust particles. However, the fine dust fraction decreases with time due to the particles coagulation. On the other hand, numeric simulations show that the collisional destruction of planetesimals is also an effective process, causing a fine dust to persist over millions of years (Birnstiel et al., 2009). Dozens of images of transitional and debris disks have been obtained by space and ground-based telescopes; see, e.g., (Padgett et al., 1999; Grady et al., 2005; Kalas et al., 2005; Mathews et al, 2012; Mayama et al., 2012; Kennedy et al., 2012). In the imaged disks, global structures are detected, namely: spiral arms (Grady et al., 2001; Hashimoto et al., 2011; Christiaens et al., 2014), ring-like gaps (Weinberger et al., 1999), bright rings (Kalas et al., 2005), inner holes (Mathews et al, 2012; Mayama et al., 2012), warps (Heap et al., 2000), density clumps (Greaves et al., 1998). Images of circumstellar disks in wide binary systems are given in (Mayama et al., 2010; Kennedy et al., 2012).

The formation of spiral waves depends on the viscous gas properties. When the gaseous component disappears, the accretion stops, and any further structure formation takes place in the planetesimal disk. In this paper, we explore the dynamical stirring of a planetesimal circumbinary disk of a binary star in the epoch when the gas component disappears. We show that the orbital precession of the particles forming the disk generates prominent spiral patterns, and we describe these patterns analytically.

It should be emphasized that, in this paper, we consider mostly the *circumbinary* disks (in which the planetesimals are moving around both stars situated at the disk center; thus the disk is an outer one with respect to the binary). *Circumstellar* disks, in which the planetesimals are moving around one of the binary components (thus the disk is an inner one), are discussed

only in brief (in Section 6).

The paper is structured as follows. In Section 2, we consider a secular theory for the dynamics of planetesimals in circumbinary disks, and derive necessary formulas for the secular evolution of the planetesimal eccentricity and longitude of pericenter. In Section 3, the radial (with respect to the central binary) secular “oscillations” of the planetesimal eccentricity are investigated analytically and compared to known results of numeric simulations. In Section 4, we consider the time evolution of individual orbits and, again, make comparisons with known results of numeric simulations. In Section 5, basing on our theory, we derive a formula for the “secular” spiral patterns in circumbinary disks, and explore correspondence between the analytical spiral pattern and the numeric-experimental density waves. In Section 6, the circumstellar case is briefly discussed. Conclusions are summarized in Section 7.

2 The secular theory

In this Section, we develop a secular theory for the dynamics of planetesimals in circumbinary disks, following theoretical approaches by Heppenheimer (1978) and Moriwaki & Nakagawa (2004). A secular perturbation theory, providing analytical formulas for the particle’s eccentricity e and the longitude of periastron ϖ , was derived by Heppenheimer (1978) (see also Whitmire et al. 1998; Thébault et al. 2006) for the circumstellar (circumprimary or circumsecondary) case. It was used to analytically describe, how a circumstellar disk of a young star is stirred by a companion star. On the other hand, the circumbinary case was considered by Moriwaki & Nakagawa (2004). They presented approximate differential equations for the secular evolution of the eccentricity vector; see Appendix in Moriwaki & Nakagawa (2004). We combine the approaches of Heppenheimer (1978) and Moriwaki & Nakagawa (2004) to derive necessary explicit analytical formulas for the secular evolution of the planetesimal eccentricity and longitude of pericenter.

Hereafter we adopt the barycentric frame; m_1 and m_2 are the masses of the binary components (we set $m_1 \geq m_2$), a_b is the binary semimajor axis, e_b is the binary eccentricity, a is the semimajor axis of the planetesimal orbit. The masses are measured in the solar units, distances in astronomical units (AU), time in years. Thus the gravitational constant G is equal to $4\pi^2$.

The *hierarchical* three-body problem “binary–planetesimal” is considered:

the distance of the planetesimal from the binary barycenter is assumed to be much greater than the size of the binary. In fact, it is superfluous to consider a non-hierarchical case, because a large central chaotic circumbinary zone exists at all eccentricities of the planetesimal, if $\mu \gtrsim 0.05$ (Shevchenko, 2014), where $\mu = m_2/(m_1 + m_2)$ is the mass parameter of the binary. This relative mass threshold has an important physical meaning (Shevchenko, 2014): above it, the tertiary (planetesimal), even starting from small eccentricities, can diffuse, following the sequence of the overlapping $p:1$ mean motion resonances between the tertiary and the binary, up to ejection from the system; close encounters with other bodies are not required for the escape. (Note that, on the other hand, in the case of inner circumstellar orbits, stable orbits always exist inside the Hill spheres of the binary components.) In what follows, we assume that $\mu \gtrsim 0.05$.

We use an averaged perturbing function expansion presented in Moriwaki & Nakagawa (2004) for the circumbinary case. This is a power-law expansion in the ratio of the binary and planetesimal semimajor axes and in the eccentricities. The expansion is up to the third order in the ratio of the semimajor axes and up to the fourth order in the eccentricities, inclusive. Note that the ratio of the binary and planetesimal semimajor axes is assumed to be small, since the hierarchical problem is considered. We integrate analytically the corresponding equations of motion (see Eqs. (A7) in Moriwaki & Nakagawa 2004), and thus straightforwardly deduce formulas for the secular evolution of the eccentricity e and the longitude of periastron ϖ of the circumbinary planetesimal. They turn out to be very similar to those in the circumstellar case, presented in Heppenheimer (1978), and read:

$$e = e_{\max} \left| \sin \frac{ut}{2} \right|, \quad (1)$$

$$\tan \varpi = -\frac{\sin ut}{1 - \cos ut}, \quad (2)$$

where t is time,

$$u = \frac{3\pi}{2} \frac{m_1 m_2}{(m_1 + m_2)^{3/2}} \frac{a_b^2}{a^{7/2}} \left(1 + \frac{3}{2} e_b^2 \right), \quad (3)$$

and $e_{\max} = 2e_f$, where e_f is the so-called forced eccentricity:

$$e_f = \frac{5(m_1 - m_2)}{4(m_1 + m_2)} \frac{a_b}{a} e_b \frac{(1 + \frac{3}{4}e_b^2)}{(1 + \frac{3}{2}e_b^2)}. \quad (4)$$

Using a new variable, namely, $y = \frac{ut}{2}$, we rewrite Eq. (2) in the form

$$\begin{aligned} \text{if } y \geq -\pi \text{ and } y \leq -\frac{\pi}{2}, \text{ then } \varpi &= y + 5\frac{\pi}{2}; \\ \text{if } y \geq -\frac{\pi}{2} \text{ and } y \leq 0, \text{ then } \varpi &= y + \frac{\pi}{2}; \\ \text{if } y \geq 0 \text{ and } y \leq \frac{\pi}{2}, \text{ then } \varpi &= y + 3\frac{\pi}{2}; \\ \text{if } y \geq \frac{\pi}{2} \text{ and } y \leq \pi, \text{ then } \varpi &= y - \frac{\pi}{2}. \end{aligned} \quad (5)$$

Thus u can be regarded as a ‘‘precession rate’’ (though in a modified fashion) of an individual orbit.

In the following Sections, we use these formulas to describe analytically the secular dynamics of planetesimals in circumbinary disks.

As opposed to the circumbinary case, in the circumstellar disks the planetesimals are moving around one of the binary components. However, in the circumstellar case, the basic expressions for the eccentricity and longitude of periastron are virtually the same: they are given by Eqs. (1), (2), and (5), but the formulas for the u and e_f parameters, entering these expressions, are different. We quote them as given in (Heppenheimer, 1978; Whitmire et al., 1998; Thébault et al., 2006), but arrange in our notations:

$$u = \frac{3\pi}{2} \frac{m_2}{m_1^{1/2}} \frac{a^{3/2}}{a_b^3} (1 - e_b^2)^{-3/2}, \quad (6)$$

$$e_f = \frac{5}{4} \frac{a}{a_b} \frac{e_b}{(1 - e_b^2)}. \quad (7)$$

Here m_1 is the primary mass (around which the particle orbits), and m_2 the perturbing mass; $m_1 > m_2$. Note that in the treatment by Heppenheimer (1978) the perturbing function is not expanded in the eccentricities, but solely in the ratio of the planetesimal and binary semimajor axes (up to the third order inclusive). The ratio of the planetesimal and binary semimajor axes is assumed to be small, since the hierarchical problem is considered.

3 Radial “oscillations” of eccentricity

Numerical simulations of the dynamical stirring of planetesimal disks on secular timescales, in various problem settings, were performed in (Moriwaki & Nakagawa, 2004; Meschiari et al., 2012a; Meschiari, 2012b; Paardekooper et al., 2012). In particular, graphs of the eccentricity and longitude of periastron of a circumbinary particle in function of its semimajor axis were constructed numerically. Let us show that such graphs can be as well constructed analytically using the theory described above.

As an actual binary example, we consider *Kepler-16*. This binary is remarkable to host the first ever discovered circumbinary planet in a double main-sequence star system. The binary’s parameters are: $m_1 = 0.69M_\odot$, $m_2 = 0.2026M_\odot$, $e_b = 0.159$, $a_b = 0.2243$ AU (Doyle et al., 2011). Analytically constructed diagrams, as given by Eqs. (1) and (5) at $t = 10^5$ yr are shown in Figure 1. Radial “waves” of eccentricity, well-known from numeric diagrams in (Moriwaki & Nakagawa, 2004; Meschiari et al., 2012a; Meschiari, 2012b; Paardekooper et al., 2012), are clearly recognizable.

Our diagrams match exactly those constructed in (Moriwaki & Nakagawa, 2004; Meschiari, 2012b) in the models with the same parameters, when the gas component is absent. A direct comparison of our diagrams with those constructed in (Meschiari et al., 2012a; Paardekooper et al., 2012) in the models with the gas component shows that the presence of gas increases the timescale of eccentricity pumping. E.g., if one adds a small portion of gas into the SPH simulation (in the model with $m_1 = M_\odot$, $m_2 = 0.2M_\odot$, $e_b = 0.4$, $a = 1$ AU), setting the sound speed $c = 5$ m/s, one finds that the timescale for the shrinking of the radial “wave” of eccentricity increases: the same level of shrinking is achieved in the models without and with gas at the times $t = 8 \cdot 10^3$ yr and $t = 10^4$ yr, respectively.

4 Time evolution of individual orbits

An analogous approach can be used to describe secular oscillations of a circumbinary orbit of a particle (a planetesimal or a planet) in dependence on time, at a fixed semimajor axis. In this respect, one can compare the theory derived above with the results of numeric simulations performed in (Leung & Lee, 2013; Dunhill & Alexander, 2013; Meschiari, 2014) for the planet *Kepler-16b*. We set the binary parameters to be the same as cited in

Section 3, and $a = 0.7016$ AU is fixed for the planet. The initial conditions for the planet motion are taken from Doyle et al. (2011).

In Figure 2, time dependences for the eccentricity and the longitude of periastron, given by Eqs. (1) and (5), are constructed. As follows from a direct comparison with the corresponding numeric-experimental graphs in (Leung & Lee, 2013; Meschiari, 2014), our secular theory formulas match these graphs perfectly.

5 Patterns in circumbinary disks

Basing on the analytical dependences of the eccentricity and the longitude of periastron on the semimajor axis (Eqs. (1) and (5)), let us proceed to investigate the circumbinary disk structure, emerging due to the secular perturbations from the central binary. As it is clear from Figure 1, the formation of structures is inevitable, because maxima of eccentricities correspond to the particles groupings at apocenters, due to the low velocities of particles there. Therefore, the disk radial densities are non-uniform at any fixed time.

Let us provide an illustrative example. Fixing the time of evolution to $t = 10^4$ binary periods, we calculate analytically the evolved planetesimal orbits in the semimajor axis a interval from $3a_b$ to $16a_b$ with the distance step $\Delta a = 0.01$. (The chosen inner radius corresponds roughly to the typical size of the circumbinary chaotic zone, see Shevchenko 2014.) The planetesimal orbits at each a are shown by dots, with the time step equal to 0.01 of the planetesimal orbital period. The binary parameters are set to be $m_1 = M_\odot$, $m_2 = 0.2M_\odot$, $e_b = 0.4$, $a = 1$ AU; this choice corresponds to the “most eccentric” model in Moriwaki & Nakagawa (2004). The resulting diagrams are presented in Figure 3a. Besides, we have performed an SPH-code numeric simulation, corresponding to this model (i.e., the parameters and initial conditions are the same). The SPH-code realized in Sotnikova (1996) has been used. The results are presented in Figure 3b. In both panels of Figure 3 spiral patterns are evident. They are tightly bound in the direction of the companion motion.

Recall that we consider the gas-free case here; if one adds the gas component, then our simulation results demonstrate that increasing the gas content slows down the wave propagation, the wave pattern remaining, however, self-similar. The spiral becomes less tightly bound; the “shrinking” of the spiral arm is slowed down by the viscosity. If the viscosity is high enough the spiral pattern does not emerge altogether.

Let us derive an analytical formula for the spiral pattern in the gas-free case. This can be done by tracing the radial distance r of the apocenter at the maximum (in the course of its secular evolution) eccentricity of particle's orbit, in function of the polar angle θ . The apocenters are attained at $\varpi = \pi \bmod 2\pi$, i.e., at the polar angle $\theta = \pi \bmod 2\pi$. At these points, the analytical solution is known (Eqs. (1) and (5)). Taking into account that at $\theta = 0 \bmod 2\pi$ the spiral corresponds to particle's minimum (zero) eccentricity, and interpolating between the consecutive points $\theta = \pi n$ ($n = 1, 2, 3, \dots$), one arrives at

$$r(\theta) = \left(\frac{At}{\theta}\right)^{2/7} + B(1 - \cos\theta), \quad (8)$$

where the constants

$$A = \frac{3\pi}{2} \frac{m_1 m_2}{(m_1 + m_2)^{3/2}} a_b^2 \left(1 + \frac{3}{2} e_b^2\right), \quad B = \frac{5}{4} \frac{m_1 - m_2}{m_1 + m_2} a_b e_b \frac{\left(1 + \frac{3}{4} e_b^2\right)}{\left(1 + \frac{3}{2} e_b^2\right)}. \quad (9)$$

Thus the pattern represents a shifted ‘‘power-law spiral’’. The main term, proportional to $\theta^{-2/7}$, represents a generalized *lituus* (a crook). (Note that the classical lituus is a little bit different, being given by $r \propto \theta^{-1/2}$.) The shifting term $\propto (1 - \cos\theta)$ represents the *cardioid*.

In Figure 4, we illustrate graphically how well our analytical spiral matches the density wave emerging in numeric simulations. Namely, we superimpose the analytical spiral on the numeric-experimental plot taken from Figure 3a. The analytical curve is given by Eq. (8); in the Figure, it is depicted by a thick solid line. A good agreement between the analytical spiral and the numeric density wave is evident.

6 Circumstellar disks

As opposed to the circumbinary case, the *circumstellar* disks are defined as those in which the planetesimals are moving around one of the binary components. Thus the disk is an inner one, with respect to the binary itself. In this Section, we briefly consider the circumstellar case.

Planetesimals orbiting a component of a binary star are subject to perturbations due to the stellar companion. The perturbations pump the eccentricities of planetesimals and inhibit their accumulation process (Marzari & Scholl,

2000; Thébault et al., 2004). In Thébault et al. (2006), the timescales for the inward propagation of the orbital crossing “wave” are calculated in gas-free models. In the more realistic models, the density wave inward propagation is damped by the gas drag and collisions.

In circumstellar disks, strong spiral arms can be present, subject to retrograde precession (Kley & Nelson, 2008; Paardekooper et al., 2008). Oscillations of planetesimal orbital parameters (the eccentricity and the longitude of pericenter) in function of time, at a fixed semimajor axis, are presented graphically in (Kley & Nelson, 2008; Marzari et al., 2009; Beaugé et al., 2010; Marzari et al., 2012; Müller & Kley, 2012; Leiva et al., 2013) for various values of disk parameters (mass, viscosity, radiative transfer properties). Numerically simulated diagrams of the eccentricity and the longitude of periastron of planetesimals in function of the semimajor axis, at a fixed time, are presented in (Marzari & Scholl, 2000; Paardekooper et al., 2008; Paardekooper & Leinhardt, 2010; Leiva et al., 2013). The choice of parameters for the simulations usually correspond to the binary systems γ Cep and α Cen, possessing circumstellar planets.

The secular evolution in the circumstellar case is described analytically by Eqs. (1), (2), (5), (6), and (7). The “secular” spiral pattern is analogous to that derived in Section 5. A detailed analysis for the circumstellar case, alongside with comparisons with the cited numerous simulation results, will be performed elsewhere.

7 Conclusions

Thus we have combined the approaches of Heppenheimer (1978) and Moriwaki & Nakagawa (2004) to derive explicit analytical formulas for the secular evolution of the eccentricities and longitudes of pericenters of planetesimals in circumbinary disks, when the gas component disappears. We have shown that, if the binary is eccentric and its components have unequal masses, spiral density waves are generated. They engulf the disk on the secular timescale. Being transient (on the secular timescale), their observed presence may betray system’s young age.

Our analytical results, given by Eqs. (1)–(5) and Eqs. (6)–(7), explain qualitatively and quantitatively many numeric-experimental diagrams, such as presented in (Marzari & Scholl, 2000; Moriwaki & Nakagawa, 2004; Thébault et al., 2006; Paardekooper et al., 2008; Paardekooper & Leinhardt, 2010; Meschiarri et al.,

2012a; Meschiari, 2012b; Paardekooper et al., 2012; Leiva et al., 2013) for the eccentricity and the longitude of periastron in function of the semimajor axis at a fixed time, as well as presented in (Marzari et al., 2009; Beaugé et al., 2010; Müller & Kley, 2012; Leung & Lee, 2013; Leiva et al., 2013; Meschiari, 2014) for the eccentricity and the longitude of periastron in function of time at a fixed semimajor axis.

For the gas-free case, we have derived an analytical formula for the spiral pattern; this formula describes a modified “lituus” (a shifted power-law spiral). Its form is in perfect agreement with our results of modeling the precessing planetesimal orbits, as well as our results of direct SPH simulations performed for the same disk parameters and initial conditions. Using the SPH scheme, we have shown that the effect of residual gas is to slow down the spiral wave propagation.

Finally, note that the derived one-armed spiral pattern is a *secular* one; i.e., it does not concern any orbital resonances. On the other hand, the presence of multi-armed spiral patterns in astrophysical disks is usually associated to Lindblad resonances; see Binney & Tremaine (2008) for the case of galactic dynamics and Murray & Dermott (1999) for the case of planetary ring dynamics. Whether multi-armed structures are possible to observe in the case of planetesimal circumbinary disks? We think that this is not possible, because all low-order resonances are deep inside the central chaotic zone around the binary (if $\mu \gtrsim 0.05$, see Shevchenko 2014). Conversely, observable multi-armed structures can be generated by resonances in the circumstellar case, i.e., in the inner disks, because the stellar companions are inside their individual stability regions.

The authors wish to thank Alice Quillen for useful remarks and comments, and Natalia Sotnikova for providing the SPH-code software. This work was supported in part by the Russian Foundation for Basic Research (projects # 14-02-00319 and # 14-02-00464) and the Programme of Fundamental Research of the Russian Academy of Sciences “Fundamental Problems of the Solar System Studies and Exploration”.

References

- Artymowicz, P., & Lubow, S. H. 1996, ApJ, 467, L77
Bate, M. R., & Bonnell, I. A. 1997, MNRAS, 285, 33

- Beugé, C., Leiva, A. M., Haghhighipour, N., & Correa Otto, J. 2010, MNRAS, 408, 503
- Binney, J., & Tremaine, S. 2008, Galactic Dynamics (2nd ed.; Princeton, PUP)
- Birnstiel, T., Dullemond, C. P., & Brauer, F. 2009, A&A, 503, L5
- Bisikalo, D. V., Boyarchuk, A. A., Kaigorodov, P. V., Kuznetsov, O. A., & Matsuda, T. 2004, ARep, 48, 449
- Christiaens, V., Casassus, S., Perez, S., et al. 2014, ApJ, 785, L12
- Clampin, M., Krist, J. E., Ardila, D. R., et al. 2003, ApJ, 126, 385
- Doyle, L. R., Carter, J. A., Fabrycky, D. C., et al. 2011, Sci, 333, 1602
- Dunhill, A. C., & Alexander, R. D. 2013, MNRAS, 435, 2328
- Grady, C. A., Polomski, E. F., Henning, Th., et al. 2001, ApJ, 122, 3396
- Grady, C. A., Woodgate, B. E., Bowers, C. W., et al. 2005, ApJ, 630, 958
- Greaves, J. S., Holland, W. S., Moriarty-Schieven, G., et al. 1998, ApJ, 506, L133
- Gunther, R., & Kley, W. 2002, A&A, 387, 550
- Hanawa, T., Ochi, Y., & Ando, K. 2010, ApJ, 708, 485
- Hashimoto, J., Tamura, M., Muto, T., et al. 2011, ApJ, 729, L17
- Heap, S. R., Lindler, D. J., Lanz, Th. M., et al. 2000, ApJ, 539, 435
- Heppenheimer, T. A. 1978, A&A, 65, 421
- Kaigorodov, P. V., Bisikalo, D. V., Fateeva, A. M., et al. 2010, ARep, 54, 1078
- Kalas, P., Graham, J. R., & Clampin, M. 2005, Natur, 435, 1067
- Kennedy, G. M., Wyatt, M. C., Sibthorpe, B., et al. 2012, MNRAS, 421, 2264

- Kley, W., & Nelson, R. P. 2008, *A&A*, 486, 617
- Leiva, A. M., Correa-Otto, J. A., & Beaugé, C. 2013, *MNRAS*, 436, 3772
- Leung, G. C. K., & Lee, M. H. 2013, *ApJ*, 763, 107
- Marzari, F., & Scholl, H. 2000, *ApJ*, 543, 328
- Marzari, F., Scholl, H., Thébault, P., & Baruteau, C. 2009, *A&A*, 508, 1493
- Marzari, F., Baruteau, C., Scholl, H., & Thébault, P. 2012, *A&A*, 539, A98
- Mathews, G. S., Williams, J. P., & Ménard, F. 2012, *ApJ*, 753, 59
- Matthews, B. C., Krivov, A. V., Wyatt, M. C., Bryden, G., & Eiroa, C. 2014, arXiv:1401.0743
- Mayama, S., Tamura, M., Hanawa, T., et al. 2010, *Sci*, 327, 306
- Mayama, S., Hashimoto, J., Muto, T., et al. 2012, *ApJ*, 760, L26
- Meschiari, S. 2012a, *ApJ*, 752, 71
- Meschiari, S. 2012b, *ApJ*, 761, L7
- Meschiari, S. 2014, *ApJ*, 790, 41
- Moriwaki, K., & Nakagawa, Y. 2004, *ApJ*, 609, 1065
- Müller, T. W. A. & Kley, W. 2012, *A&A*, 539, A18
- Murray, C. D., & Dermott, S. F. 1999, *Solar System Dynamics* (Cambridge, CUP)
- Mustill, A. J., & Wyatt, M. C. 2009, *MNRAS*, 399, 1403
- Nelson, A. F. 2000, *ApJ*, 537, L65
- Ochi, Y., Sugimoto, K., & Hanawa, T. 2005, *ApJ*, 623, 922
- Paardekooper, S.-J., Thébault, P., & Mellema, G. 2008, *MNRAS*, 386, 973
- Paardekooper, S.-J. & Leinhardt, Z. M. 2010, *MNRAS*, 403, L64

- Paardekooper, S.-J., Leinhardt, Z. M., Thébault, T., & Baruteau, C. 2012, ApJ, 754, L16
- Padgett, D. L., Brandner, W., Stapelfeldt, K. R., et al. 1999, ApJ, 117, 1490
- Picogna, G., & Marzari, F. 2013, A&A, 556, A148
- Shevchenko, I. I. 2014, arXiv:1405.3788.
- Sotnikova, N. Ya. 1996, Ap, 39, 141
- Sotnikova, N. Ya., & Grinin, V. P. 2007, AstL, 33, 594
- Thébault, P., Marzari, F., Scholl, H., Turrini D., & Barbieri, M. 2004, A&A, 427, 1097
- Thébault, P., Marzari, F., & Scholl, H., 2006, Icar, 183, 193
- Weinberger, A. J., Becklin, E. E., Schneider, G., et al. 1999, ApJ, 525, L53
- Whitmire, D., Matese, J., Criswell, L., & Mikkola, S. 1998, Icar, 132, 196
- Wyatt, M. C. 2005, A&A, 440, 937

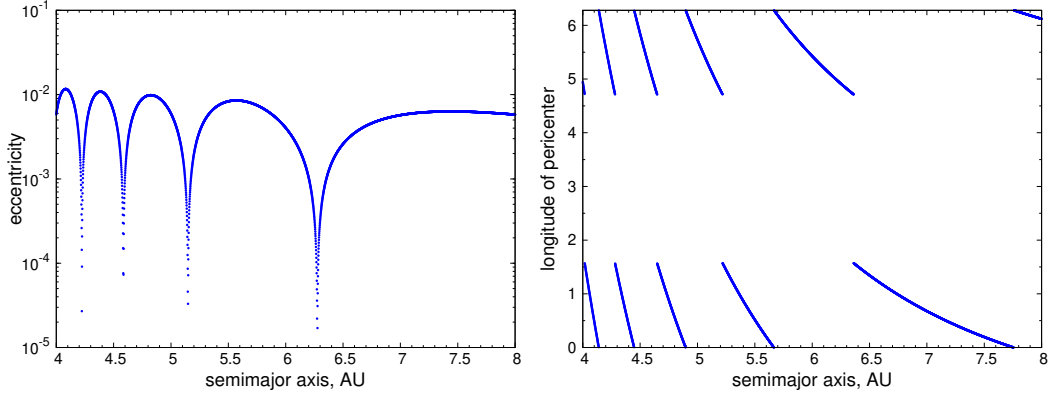


Figure 1: The secular eccentricity “waves” (left) and the secular behavior of the longitude of pericenter (right) of planetesimals in a model disk, in function of the semimajor axis at a fixed time. For the model parameters see text. (A color version of this figure is available in the online journal.)

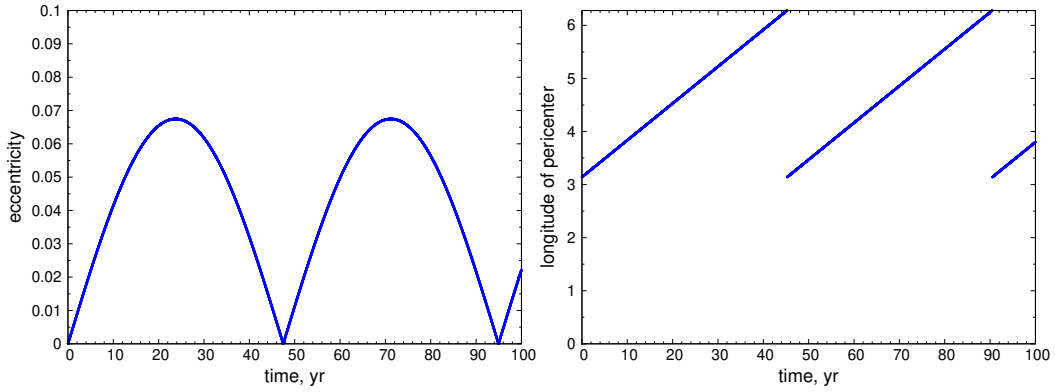


Figure 2: The eccentricity secular oscillations (left) and the longitude-of-pericenter secular rotation (right) in case of *Kepler-16b*, in function of time at a fixed semimajor axis. (A color version of this figure is available in the online journal.)

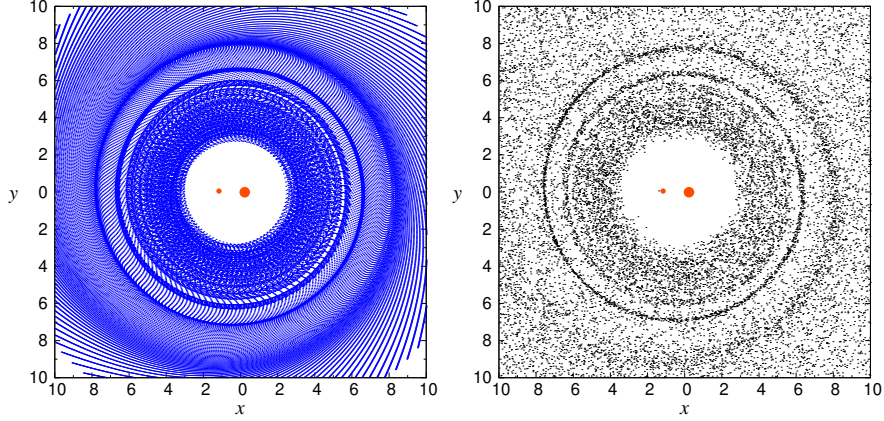


Figure 3: A spiral pattern in a model planetesimal disk. The set of precessing orbits, constructed analytically (left), and the corresponding SPH simulation (right). The model parameters: $m_1 = M_\odot$, $m_2 = 0.2M_\odot$, $e_b = 0.4$, $a = 1$ AU, $t = 10^4$ yr. (A color version of this figure is available in the online journal.)

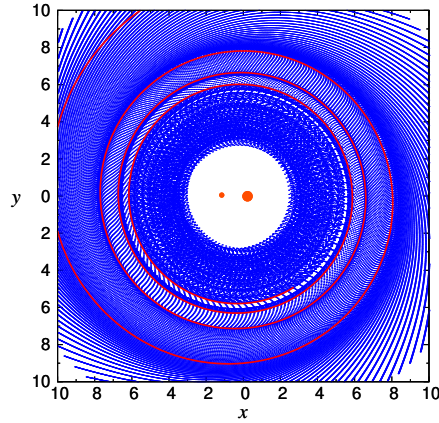


Figure 4: The plot of Figure 3a with the analytical spiral curve superimposed. The latter is given by Eq. (8) and is depicted by a thick solid line. (A color version of this figure is available in the online journal.)